Catalysis Letters
https://doi.org/10.1007/s10562-021-03567-y

Theoretical Investigation of the Size Effect on the Oxygen Adsorption Energy of Coinage Metal Nanoparticles

Amir H. Hakimioun[1] · Elisabeth M. Dietze[1,5] · Bart D. Vandegehuchte[3] · Daniel Curulla-Ferre[3] · Lennart Joos[4] · Philipp N. Plessow[1] · Felix Studt[1,2]

Received: 16 November 2020 / Accepted: 10 February 2021

Abstract

This study evaluates the finite size effect on the oxygen adsorption energy of coinage metal (Cu, Ag and Au) cuboctahedral nanoparticles in the size range of 13 to 1415 atoms (0.7–3.5 nm in diameter). Trends in particle size effects are well described with single point calculations, in which the metal atoms are frozen in their bulk position and the oxygen atom is added in a location determined from periodic surface calculations. This is shown explicitly for Cu nanoparticles, for which full geometry optimization only leads to a constant offset between relaxed and unrelaxed adsorption energies that is independent of particle size. With increasing cluster size, the adsorption energy converges systematically to the limit of the (211) extended surface. The 55-atomic cluster is an outlier for all of the coinage metals and all three materials show similar behavior with respect to particle size.

Graphic Abstract

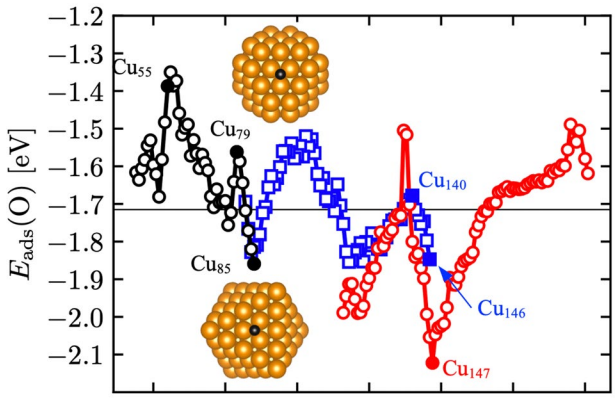

Keywords Size effect · Coinage metals · DFT · Oxygen adsorption

Amir H. Hakimioun and Elisabeth M. Dietze have contributed equally to this article.

✉ Felix Studt
felix.studt@kit.edu

[1] Institute of Catalysis Research and Technology (IKFT), Hermann-von-Helmholtz-Platz 1, 76344 Eggenstein-Leopoldshafen, Germany

[2] Institute for Chemical Technology and Polymer Chemistry, Karlsruhe Institute of Technology, 76131 Karlsruhe, Germany

[3] Total Research & Technology Feluy, B-7181 Seneffe, Belgium

[4] Barkenlaan 66, B-8660 De Panne, Belgium

[5] Department of Physics and Competence Centre for Catalysis, Chalmers University of Technology, 41296 Göteborg, Sweden

Published online: 26 February 2021

Transition metal nanoparticles are widely used in heterogenous catalysis for a broad variety of reactions ranging from hydrogenation to emission control, with nanoparticle sizes typically ranging from 3–20 nm. [1–3] While smaller particles have a higher specific surface area per gram of catalyst, they are often unstable and tend to sinter to larger particles during application. [4, 5] Interestingly, it has been reported that smaller sizes lead not only to larger catalytic surface areas and higher concentrations of various surface terminations, but could also exhibit different catalytic properties. Perhaps the most striking example is given by gold nanoparticles that have been shown to be highly active for CO oxidation while gold is otherwise not active at all. [6–8] These strong deviations of smaller clusters and particles from bulk-like behavior are often denoted as 'quantum size effects' and are due to the vanishing of the d-band into more localized, atomic-like d-states. [9, 10] The size effect has been investigated theoretically for gold [9, 11] and platinum [10] nanoparticles up to the size of 3.7 nm. The transition of the underlying electronic structure towards the bulk limit has been identified at around 2.5 nm at which point the adsorption energies of O and CO converge to the limit of extended surfaces accompanied by the formation of a d-band. Other studies of the effect of the particle size on adsorption energies included Pt [12, 13] and Pd [14, 15]. Apart from gold, copper and silver are highly interesting transition metals with applications in methanol synthesis, [16–18] the water–gas-shift reaction [19] and selective oxidation [20, 21]. Particle size effects have also been identified for copper experimentally (e.g. for methanol synthesis), [22] but theoretical studies exist only for smaller copper clusters (< 1 nm). [23–31] Similarly, experimental data for Ag demonstrated a strong size dependency for ethylene epoxidation [32, 33], but only small Ag clusters have been studied theoretically to date. [34].

In this work, we investigate the effect of particle size for all three coinage metals, Cu, Ag and Au using density functional theory (DFT) calculations. As particles that are relevant for catalysis are typically larger than 1 nm for Cu [22] Ag [35] and Au [6], we are particularly interested in particle size effects including these sizes. While particles are mostly supported in heterogeneous catalysis, we investigate free standing particles. This has the advantage of decoupling particle size effects from perturbations of a particular support in addition to being computationally more feasible. We therefore note that a direct comparison with experiments would need to account for metal-support interactions in addition to size effects. We focus on the oxygen adsorption energy, that has been shown to be a key descriptor in the hydrogenation of CO_2 to methanol, [36] using cuboctahedral nanoparticles ranging from 13 to 1415 atoms (0.7–3.5 nm in diameter, see Fig. 1). The clusters are chosen such that we can systematically investigate the size effect while

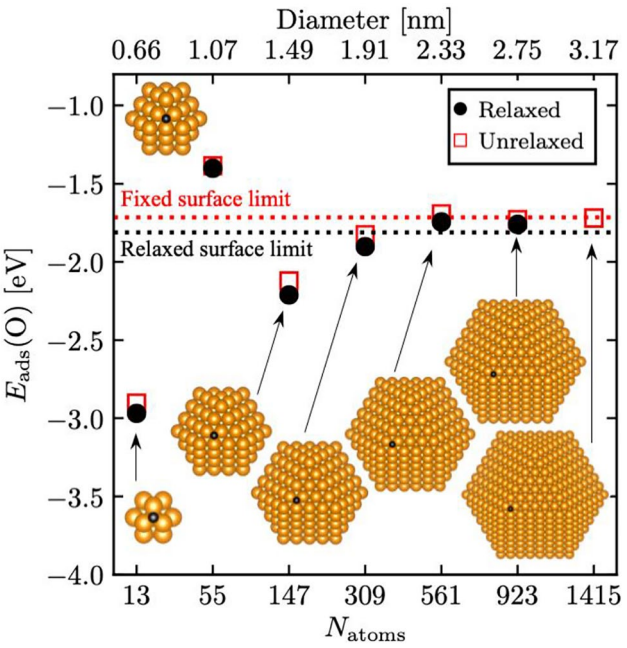

Fig. 1 Adsorption energy of oxygen (relative to ½ gas phase O_2) on various fully optimized (black filled circles) and unrelaxed (red empty squares) Cu nanoparticles as a function of the number of atoms within the nanoparticles (N_{atoms}). The upper abscissa gives the corresponding nanoparticle diameter in nm derived from spherical particles (see SI). The surface limit of the relaxed nanoparticles is given as a black dotted line and the corresponding limit for the fixed geometry as a red dotted line as calculated for adsorption on the fcc site of a Cu(211) slab with a coverage of 1/9. As insets, all Cu nanoparticles with adsorbed oxygen (black) are shown

maintaining the shape of the cluster and the adsorption site of the oxygen. We employ the BEEF-vdW functional [37] to calculate the oxygen adsorption energy on the fcc adsorption position closest to the corner of the (111) facet of the nanoparticles such that the adsorption site is the same for all particles with the exception of M_{13}, as shown in the insets in Fig. 1. For Cu, the effect of geometry optimization is studied explicitly. For free standing metal Cu clusters ranging from 13 to 923 atoms, a linear relation between the mean Cu-Cu distance, the chemical potential which is approximated by the average energy per atom, and the number of atoms to the power of -1/3 (see Figure S3) is observed, similarly to what has been found for other metals [13, 34, 38–45]. Figure 1 shows the adsorption energy of an oxygen atom on the Cu clusters with increasing size. The filled black circles show the results of the optimized structures. It can be seen that the adsorption energy converges to the limit of the Cu(211) surface for Cu_{309} and larger. As previously seen for Au_{55}, Cu_{55} shows a comparatively weak adsorption energy for oxygen. Comparing these results to single point calculations, using the Cu bulk lattice constant and the copper-oxygen distance obtained from Cu(111) surface calculations, it can be seen that all adsorption energies are shifted to higher values by

approximately 0.1 eV. Keeping in mind that the accuracy of the BEEF-vdW functional with respect to adsorption energies on transition metal surfaces is around 0.2 eV, [46] the constant shift implies that the effect of strain is small and similar for all clusters, which can be also seen in Figure S4 which plots the adsorption energy of oxygen on strained Cu(111) surfaces. This is in agreement with Kleis et al. [9] and Li et al. [10], who found that trends in adsorption energies are similar for relaxed and unrelaxed clusters for Au and Pt. As was shown before by Mavrikakis et al. [47] and others [48–50], the overall effect of strain is usually linear for up to 3% deviation [51] from the lattice constant.

Figure 2 compares the oxygen adsorption energy on unrelaxed Cu, Ag and Au nanoparticles, showing that for the 309-atomic cluster adsorption energies are converged to within about 0.2 eV. Interestingly, all three coinage metals follow the exact same trend, that is (1) strong adsorption on M_{13}, (2) weakest adsorption on M_{55}, (3) again stronger binding on M_{147} and (4) slow convergence from M_{309} and M_{561} towards the bulk limit. Overall, there is a systematic offset between the binding energies of a given cluster for the three metals, with binding energies generally decreasing from Cu over Ag to Au.

Li et al. [52] argued that quantum size effects play a significant role for platinum clusters below 2 nm. This has been attributed to a change from a broad d-band to more discrete d-states, as the extent of orbital overlap of individual atoms decreases.

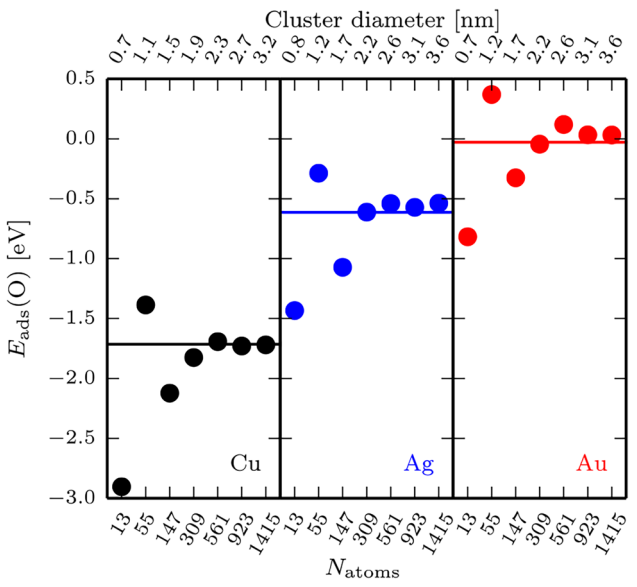

Fig. 2 Adsorption energy of oxygen (relative to ½ gas phase O_2) on unrelaxed Cu, Ag and Au nanoparticles versus the number of atoms. The upper abscissa shows the corresponding nanoparticle diameter. The lines are the surface limit for adsorption on the fcc-site on the fixed 211-slab of the corresponding metal

So far, our study only includes geometric closed-shell cuboctahedral clusters [53], which can be generated by sequentially adding coordination shells starting from a single atom, resulting in a monotonic increase of cluster sizes by increments of about 0.4–0.5 nm. In order to investigate the size effect for smaller variations in more detail we investigated Cu nanoparticles ranging from 44 to 200 atoms as shown in Fig. 3a. These clusters have been derived from cuboctahedral Cu_{55}, octahedral Cu_{146}, and cuboctahedral Cu_{147} by adding or removing atoms to or from the fcc lattice positions to create stable intermediate clusters. In particular, the atoms with lowest coordination number were removed first or atoms were added so that the added atom has the highest possible coordination number. In case of different options for adding or removing atoms with the same coordination number, the site associated with the largest vertical distance from the top facet was chosen to minimize the direct influence on the oxygen adsorption site. For example, for cuboctahedral particles, atoms were first added to the fcc(100) sites towards the formation of octahedral particles (the coordinates of all structures are given in the SI). It can be seen that the oxygen adsorption energy varies strongly with the number of atoms and is oscillating for every 20–40 atoms. This can be explained by the so-called electronic magic numbers occurring for 58, 92 and 138 electrons, where closed-shell configurations are reached for spherical jellium clusters. [45] For the electronic configuration of coinage metals ($d^{10}s^1$), considering only the single s-electron per atom, particularly stable clusters are thus reached for cluster sizes $N_{atoms} = 58$, 92 and 138, e.g. cluster sizes with the number of atoms equal to the number of electrons in the closed-shell jellium configurations. Larsen et al. [12] have shown that for Cu, Ag and Au, clusters are particularly stable around these numbers and demonstrated that Au clusters show an increased oxygen adsorption energy. We observe a similar behavior in the oxygen adsorption energy for Cu, which shows a maximum close to these electronic magic numbers. Quantum size effects do hence play a key role for small Cu clusters where the oxygen adsorption energies change quite drastically with the addition or removal of a few copper atoms. Note also that the weak adsorption of Cu_{55} as well as the rather strong adsorption of Cu_{147} are close to the corresponding minimum and maximum. The drastic change in oxygen adsorption also means that for example Cu_{147} has a strong adsorption of about 2.1 eV, but that this is reduced by 0.4 eV when going to Cu_{140}. Atomically precise control of the particle size and size distribution would therefore be necessary if one wanted to adjust the oxygen binding energies within a narrow range. Interestingly, the behavior is very similar for Ag and Au, that follow the trends in oxygen chemisorption energies observed for copper in the 50–200 atoms range. As shown in Fig. 3b, the stability of the metal clusters follows the usual increasing

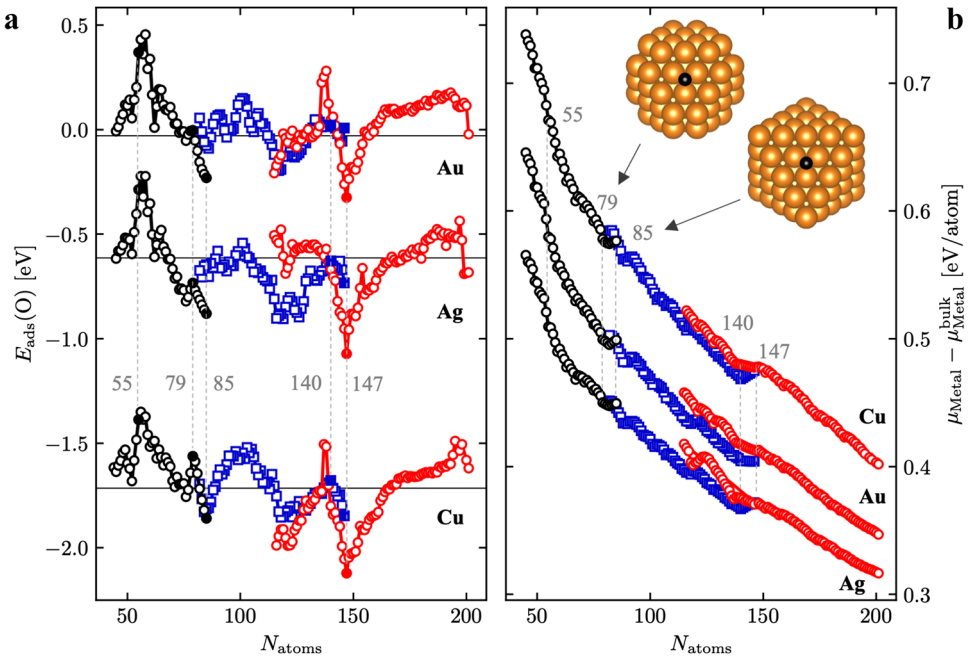

Fig. 3 **a** Oxygen adsorption energy (relative to ½ O_2 in the gas phase) on various Cu, Ag and Au fixed geometry nanoparticles as a function of particle size. **b** Chemical potential μ_M relative to the bulk chemical potential of M, μ^{bulk}_{CM} for M = Cu, Ag, Au as function of the number of atoms. The filled black circles correspond to the M_{55} cuboctahedral cluster, the M_{79} truncated octahedral and the M_{85} octahedral cluster respectively. The filled red circle corresponds to the M_{147} cuboctahedral cluster. The filled blue squares correspond to the octahedral M_{146} and truncated octahedral M_{140} clusters. The open circles and open squares correspond to clusters that can be derived from the parent clusters described above by adding or removing atoms in bulk fcc-positions. The insets show the atomic structure of oxygen adsorption (black atom) on octahedral Cu_{85} and truncated octahedral Cu_{79}

trend with cluster size, further highlighting the difficulties in precise cluster synthesis and stabilization in the reported range. Synthesis techniques such as wet impregnation or colloidal synthesis are presently not able to achieve such a high atom specificity [54] and further improvement is needed for the future design and preparation of nanoparticles.

In summary, we investigated the effect of particle size on the adsorption energy of oxygen on the coinage metals Cu, Ag and Au. We found that the effect of surface relaxation on oxygen adsorption is relatively small compared to the changes with particle size, thus allowing the use of less expensive single point calculations and thus larger particles to capture the trends in adsorption energies. Interestingly, all three metals follow the exact same trend, where adsorption is strongest for M_{13}, weakest for M_{55} and approaches smoothly the bulk limit for M_{309}/M_{561}. In contrast, changes are quite drastic for smaller clusters for which an increase or decrease by one atom in a copper cluster changes the oxygen adsorption energy by as much as 0.1 eV. While it is interesting to note that we found the exact same trend for all three coinage metals, future work will show how this relates for other transition metals as well as how support interactions impact the oxygen adsorption energy.

Supplementary Information The online version contains supplementary material available at https://doi.org/10.1007/s10562-021-03567-y.

Acknowledgement E.M.D., P.N.P and F.S. acknowledge support by the state of Baden- Württemberg through bwHPC (bwunicluster and JUSTUS, RV bw17D011). Part of this work was performed on the supercomputer ForHLR funded by the Ministry of Science, Research and the Arts Baden-Württemberg and by the Federal Ministry of Education and Research. Financial support from the Helmholtz Association is also gratefully acknowledged. Part of this work has been carried out in the framework of the Consortium on Metal Nanocatalysis funded by Total Refining & Chemicals, and it was supported by the Research Program Agreement, with reference Total/IPA-5441 between Total Research & Technology Feluy and Karlsruhe Institute of Technology (KIT).

Authors Contribution The manuscript was written through contributions of all authors. All authors have given approval to the final version of the manuscript.

Funding Open Access funding enabled and organized by Projekt DEAL.

References

1. Ertl G, Knözinger H, Schüth F, Weitkamp J (2008) Handbook of heterogeneous catalysis. Wiley, New Jersey
2. Mizuno N, Misono M (1998) Chem Rev 98:199–218
3. Bell AT (2003) Science 299:1688–1691
4. Bartholomew C (2005) Farrauto R Catalyst Deactivation: Causes, Mechanisms, and Treatment. John Wiley & Sons Inc, Hoboken, NJ
5. Xu Q, Kharas KC, Croley BJ, Datye AK (2011) ChemCatChem 3:1004–1014
6. Valden M, Lai X, Goodman DW (1998) Science 281:1647–1650
7. Bond GC, Thompson DT (1999) Catal Rev 41:319–388
8. Haruta M, Kobayashi T, Sano H, Yamada N (1987) Chem Lett 16:405–408
9. Kleis J, Greeley J, Romero N, Morozov V, Falsig H, Larsen AH, Lu J, Mortensen JJ, Dułak M, Thygesen KS (2011) Catal Lett 141:1067–1071
10. Li L, Abild-Pedersen F, Greeley J, Nørskov JK (2015) J Phys Chem Lett 6:3797–3801
11. Liu JX, Filot IAW, Su Y, Zijlstra B, Hensen EJM (2018) J Phys Chem C 122:8327–8340
12. Larsen AH, Kleis J, Thygesen KS, Nørskov JK, Jacobsen KW (2011) Phys Rev B 84:245429
13. Laletina SS, Mamatkulov M, Shor EA, Kaichev VV, Genest A, Yudanov IV, Rösch N (2017) J Phys Chem C 121:17371–17377
14. Yudanov IV, Genest A, Schauermann S, Freund H-J, Rösch N (2012) Nano Lett 12:2134–2139
15. Fischer-Wolfarth J-H, Farmer JA, Flores-Camacho JM, Genest A, Yudanov IV, Rösch N, Campbell CT, Schauermann S, Freund H-J (2010) Phys Rev B 81:241416
16. Hansen JB, Nielsen PEH (2008) In: Ertl G, Knözinger H, Schüth F, Weitkamp J (eds) Handbook of Heterogeneous Catalysis. Wiley-VCH, Weinheim Germany
17. Behrens M, Studt F, Kasatkin I, Kuhl S, Havecker M, Abild-Pedersen F, Zander S, Girgsdies F, Kurr P, Kniep BL, Tovar M, Fischer RW, Nørskov JK, Schlögl R (2012) Science 336:893–897
18. Hansen PL, Wagner JB, Helveg S, Rostrup-Nielsen JR, Clausen BS, Topsoe H (2002) Science 295:2053–2055
19. Hinrichsen K-O, Kochloefl K, Muhler M (2008). In: Ertl G, Knözinger H, Schüth F, Weitkamp J (eds) Handbook of Heterogeneous Catalysis. Wiley-VCH, Weinheim Germany
20. Mallat T, Baiker A (2008). In: Ertl G, Knözinger H, Schüth F, Weitkamp J (eds) Handbook of Heterogeneous Catalysis. Wiley-VCH, Weinheim Germany
21. Weissermel K, Arpe H-J (1993) Industrial Organic Chemistry. VCH, New York
22. van den Berg R, Prieto G, Korpershoek G, van der Wal LI, van Bunningen AJ, Laegsgaard-Jorgensen S, de Jongh PE, de Jong KP (2016) Nat Commun 7:13057
23. Yang B, Liu C, Halder A, Tyo EC, Martinson ABF, Seifer S, Zapol P, Curtiss LA, Vajda S (2017) J Phys Chem C 121:10406–10412
24. Ma L, Akola J (2019) Phys Chem Chem Phys 21:11351–11358
25. Peredkov S, Peters S, Al-Hada M, Erko A, Neeb M, Eberhardt W (2016) Catal Sci Technol 6:6942–6952
26. Dononelli W, Kluner T (2018) Faraday Discuss 208:105–121
27. Blandez JF, Primo A, Asiri AM, Alvaro M, Garcia H (2014) Angew Chem Int Ed 53:12581–12586
28. Han Y, Lai KC, Lii-Rosales A, Tringides MC, Evans JW, Thiela PA (2019) Surf Sci 685:48–58
29. Reske R, Mistry H, Behafarid F, Roldan Cuenya B, Strasser P (2014) J Am Chem Soc 136:6978–6986
30. Delley B, Ellis DE, Freeman AJ, Baerends EJ, Post D (1983) Phys Rev B 27:2132–2144
31. Zhang X, Liu JX, Zijlstra B, Filot IAW, Zhou Z, Sun S, Hensen EJM (2018) Nano Energy 43:200–209
32. Christopher P, Linic S (2010) ChemCatChem 2:78–83
33. Bukhtiyarov VI, Carley AF, Dollard LA, Roberts MW (1997) Surf Sci 381:L605–L608
34. Tsuneda T (2019) J Comput Chem 40:206–211
35. Wei H, Gomez C, Liu J, Guo N, Wu T, Lobo-Lapidus R, Marshall CL, Miller JT, Meyer RJ (2013) J Catal 298:18–26
36. Studt F, Sharafutdinov I, Abild-Pedersen F, Elkjær CF, Hummelshøj JS, Dahl S, Chorkendorff I, Nørskov JK (2014) Nat Chem 6:320
37. Wellendorff J, Lundgaard KT, Møgelhøj A, Petzold V, Landis DD, Nørskov JK, Bligaard T, Jacobsen KW (2012) Phys Rev B 85:235149
38. Dietze EM, Plessow PN, Studt F (2019) J Phys Chem C 123:25464–25469
39. Nava P, Sierka M, Ahlrichs R (2003) Phys Chem Chem Phys 5:3372–3381
40. Soini TM, Ma X, Üzengi Aktürk O, Suthirakun S, Genest A, Rösch N (2016) Surf Sci 643:156–163
41. Häberlen OD, Chung S-C, Stener M, Rösch N (1997) J Chem Phys 106:5189–5201
42. Köhn A, Weigend F, Ahlrichs R (2001) Phys Chem Chem Phys 3:711–719
43. Nanba Y, Ishimoto T, Koyama M (2017) J Phys Chem C 121:27445–27452
44. Marchal R, Yudanov IV, Matveev AV, Rösch N (2013) Chem Phys Lett 578:92–96
45. Weigend F, Ahlrichs R (2010) Philos Trans R Soc A 368:1245–1263
46. Wellendorff J, Silbaugh TL, Garcia-Pintos D, Nørskov JK, Bligaard T, Studt F, Campbell CT (2015) Surf Sci 640:36–44
47. Mavrikakis M, Hammer B, Nørskov JK (1998) Phys Rev Lett 81:2819–2822
48. Pingel TN, Jørgensen M, Yankovich AB, Grönbeck H, Olsson E (2018) Nat Commun 9:2722
49. Calle-Vallejo F, Bandarenka AS (2018) ChemSusChem 11:1824–1828
50. Jørgensen M, Grönbeck H (2019) Top Catal 62:660–668
51. Escudero-Escribano M, Malacrida P, Hansen MH, Vej-Hansen UG, Velázquez-Palenzuela A, Tripkovic V, Schiøtz J, Rossmeisl J, Stephens IEL, Chorkendorff I (2016) Science 352:73
52. Li L, Larsen AH, Romero NA, Morozov VA, Glinsvad C, Abild-Pedersen F, Greeley J, Jacobsen KW, Nørskov JK (2012) J Phys Chem Lett 4:222–226
53. Näher U, Zimmermann U, Martin TP (1993) J Chem Phys 99:2256–2260
54. Sharapa DI, Doronkin DE, Studt F, Grunwaldt JD, Behrens S (2019) Adv Mater 31:1807381